AD-A260 437

College of Earth and Mineral Sciences

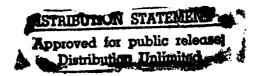PENNSTATE

A NEW INDEX FOR THE CREVICE CORROSION RESISTANCE OF MATERIALS

Yuan Xu and Howard W. Pickering

Department of Materials Science and Engineering
The Pennsylvania State University
University Park, PA 16802

DTIC
ELECTE
FEB 0 8 1993
S E D

93-02185

93   2   8   0317

PENN STATE
College of Earth and Mineral Sciences

Undergraduate Majors

Ceramic Science and Engineering, Fuel Science, Metals Science and Engineering, Polymer Science; Mineral Economics; Mining Engineering, Petroleum and Natural Gas Engineering; Earth Sciences, Geosciences; Geography; Meteorology.

Graduate Programs and Fields of Research

Ceramic Science and Engineering, Fuel Science, Metals Science and Engineering, Polymer Science; Mineral Economics; Mining Engineering, Mineral Processing, Petroleum and Natural Gas Engineering; Geochemistry and Mineralogy, Geology, Geophysics; Geography; Meteorology.

Universitywide Interdisciplinary Graduate Programs Involving EMS Faculty and Students

Earth Sciences, Ecology, Environmental Pollution Control Engineering, Mineral Engineering Management, Solid State Science.

Associate Degree Programs

Metallurgical Engineering Technology (Shenango Valley Campus).

Interdisciplinary Research Groups Centered in the College

C. Drew Stahl Center for Advanced Oil Recovery, Center for Advanced Materials, Coal Research Section, Earth System Science Center, Mining and Mineral Resources Research Institute, Ore Deposits Research Group.

Analytical and Characterization Laboratories (Mineral Constitution Laboratories)

Services available include: classical chemical analysis of metals and silicate and carbonate rocks; X-ray diffraction and fluorescence; electron microscopy and diffraction; electron microprobe analysis; atomic absorption analysis; spectrochemical analysis; surface analysis by secondary ion mass spectrometry (SIMS); and scanning electron microscopy (SEM).

REPORT DOCUMENTATION PAGE

Public reporting burden for this collection of information is estimated to average 1 hour per response, including the time for reviewing instructions, searching existing data sources, gathering and maintaining the data needed, and completing and reviewing the collection of information. Send comments regarding this burden estimate or any other aspect of this collection of information, including suggestions for reducing this burden, to Washington Headquarters Services, Directorate for Information Operations and Reports, 1215 Jefferson Davis Highway, Suite 1204, Arlington, VA 22202-4302, and to the Office of Management and Budget, Paperwork Reduction Project (0704-0188), Washington, DC 20503.

1. AGENCY USE ONLY (Leave blank)	2. REPORT DATE February 1993	3. REPORT TYPE AND DATES COVERED Technical

4. TITLE AND SUBTITLE

A New Index for the Crevice Corrosion Resistance of Materials

5. FUNDING NUMBERS

C: N00014-91-J-1189
PR: 431 5098

6. AUTHOR(S)

Yuan Xu and Howard W. Pickering

7. PERFORMING ORGANIZATION NAME(S) AND ADDRESS(ES)

The Pennsylvania State University
Department of Materials Science & Engineering
326 Steidle Building
University Park, PA 16802

8. PERFORMING ORGANIZATION REPORT NUMBER

9. SPONSORING/MONITORING AGENCY NAME(S) AND ADDRESS(ES)

Scientific Officer
Materials Division Code: 1131M
Office of Naval Research
Arlington, VA 22217-5000
ATTN: A. John Sedriks

10. SPONSORING/MONITORING AGENCY REPORT NUMBER

11. SUPPLEMENTARY NOTES

12a. DISTRIBUTION/AVAILABILITY STATEMENT

Approved for public release; distribution is unlimited.

12b. DISTRIBUTION CODE

13. ABSTRACT (Maximum 200 words)

Recent studies have revealed the crucial role played by the macro corrosion cell (potential coupling between the inside and outside of a cavity) in crevice and pitting corrosion. It was found that acidification and the existence of chloride ions in the local cell are not the sole and necessary conditions for localized corrosion to occur, and that their accelerating effects on crevice corrosion and pit growth can be explained within the frame work of the macro cell (the IR drop mechanism). Upon analysis of the results of the experiments, quantitative modeling, and the literature, a new characteristic parameter - the critical distance into the crevice, d_c - has been suggested for indexing the crevice corrosion resistance of a material under specified conditions. The advantages of using d_c as the index of the crevice corrosion resistance are: (1) it may be obtained through experiment and may also be estimated through computational approaches; (2) it has a distinct and straightforward physical meaning; (3) it may be employed in engineering design and (4) it is a single parameter which can reflect the integrated influence of several factors known to affect the crevice corrosion resistance of a material from past practical experience and research work. Preliminary work has shown good agreement between the measured and the computed values of d_c. The experimental technique and the principle of the mathematical approach to obtain d_c are described.

14. SUBJECT TERMS

Key words: quantitative test, predictive method, accelerated test, corrosion testing, crevice corrosion susceptibility

15. NUMBER OF PAGES

17. SECURITY CLASSIFICATION OF REPORT	18. SECURITY CLASSIFICATION OF THIS PAGE	19. SECURITY CLASSIFICATION OF ABSTRACT	20. LIMITATION OF ABSTRACT
UNCLASSIFIED	UNCLASSIFIED	UNCLASSIFIED	

Yuan Xu[1] and Howard W. Pickering[2]

A NEW INDEX FOR THE
CREVICE CORROSION RESISTANCE OF MATERIALS

ABSTRACT: Recent studies have revealed the crucial role played by the macro corrosion cell (potential coupling between the inside and outside of a cavity) in crevice and pitting corrosion. It was found that acidification and the existence of chloride ions in the local cell are not the sole and necessary conditions for localized corrosion to occur, and that their accelerating effects on crevice corrosion and pit growth can be explained within the frame work of the macro cell (the IR drop mechanism). Upon analysis of the results of the experiments, quantitative modeling, and the literature, a new characteristic parameter - the critical distance into the crevice, d_c - has been suggested for indexing the crevice corrosion resistance of a material under specified conditions. The advantages of using d_c as the index of the crevice corrosion resistance are: (1) it may be obtained through experiment and may also be estimated through computational approaches; (2) it has a distinct and straightforward physical meaning; (3) it may be employed in engineering design and (4) it is a single parameter which can reflect the integrated influence of several factors known to affect the crevice corrosion resistance of a material from past practical experience and research work. Preliminary work has shown good agreement between the measured and the computed values of d_c. The experimental technique and the principle of the mathematical approach to obtain d_c are described.

Keywords: quantitative test, predictive method, accelerated test, corrosion testing, crevice corrosion susceptibility

---

[1] Singapore Institute of Standards and Industrial Research (SISIR), Metal and Advanced Materials Center, Science Park Drive, Singapore 0511

[2] Department of Materials Science and Engineering
The Pennsylvania State University, University Park, PA 16802, USA

INTRODUCTION

Numerous crevice corrosion testing methods have been proposed and used with varying success. ASTM Specification G78 provides guidance in the conduct of crevice corrosion tests for stainless steels and related nickel-base alloys in sea-water and other chloride-containing environments [1], although it does not provide any particular test technique. The large amount of testing methods may be divided into two major groups. The first includes those methods which involve the use of artificial crevices. Samples with artificial crevices are immersed into the testing solution for a period of time. The crevice corrosion resistance is evaluated by the number of crevices which are found to have been corroded during the test. The spool specimen test racks [2], Ferric chloride tests [3], the Materials Technology Institute Tests (MTI-1 to MTI-5) [4] and Multiple-Crevice Assembly Testing [5] fall in this group. Among these, the Multiple-Crevice Assembly Testing [5] is the most often used. The other group employs electrochemical techniques. It includes two ASTM standard methods, ASTM G61 for iron-, nickel- and cobalt-based alloys [6] and ASTM F746 for metallic surgical implant materials [7], as well as other methods, e.g., potentiostatic test [8]; potentiodynamic test [9] and remote crevice assemblies test [10]. Although each of the techniques has its own merits and has been used with varying success, the currently used testing methods have several common problems. For instance, the data obtained through one of these tests can only serve the purposes of comparison and screening but can not be used directly for quantitative engineering design. Another problem is that data obtained by the different methods are not convertible to each other. Therefore, no method can be claimed to be the best. The reason for this may lie in the lack of a generally recognised theory on crevice corrosion so that it is difficult to link the method itself and the obtained data with the crevice corrosion mechanism.

In the present paper, a brief introduction on the progress of the mechanistic study of crevice corrosion is given first. Based on the new progress, a characteristic parameter, d_c - the critical distance into the crevice - is proposed to index the crevice corrosion resistance of a metal. The advantages for using d_c are discussed. The suggested experimental technique and the mathematical approach for obtaining d_c are described.

PROGRESS ON THE UNDERSTANDING OF CREVICE CORROSION

Two major mechanisms on crevice corrosion have been proposed. The one based on the solution composition change within crevices [e.g. 11] suggests that the hydrolysis of dissolved metal ions increases the acidity (lowers the pH) and the resulting autocatalytic effect increases appreciably the metal dissolution rate (causing crevice corrosion). However, how the so called autocatalytic effect can increase the corrosion rate within a crevice has never been explained. As a matter of fact, the actual metal dissolution rate measured in an acidified solution (equivalent to the hydrolysed crevice electrolyte solution) is far less than the observed crevice corrosion current density. Furthermore, crevice corrosion sometimes occurs in the absence of a pH decrease. Another mechanism, the IR-drop mechanism [12-13] focuses on the macro corrosion cell between the active crevice wall and the passivated sample's outer surface where the (cathodic) reduction of oxygen occurs. Or, in a potentiostatic test, the cathodic reduction occurs at the
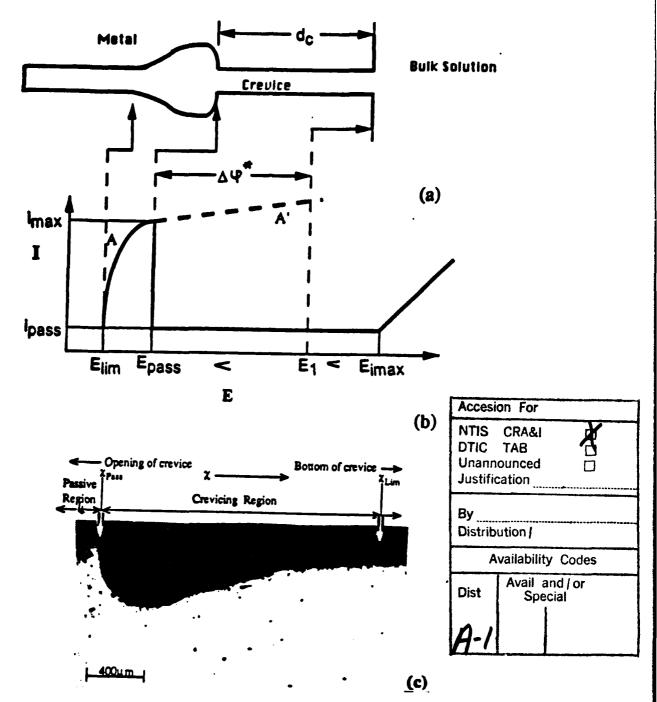
(a)

(b)

(c)

Fig. 1 (a) A crevice undergoing corrosion below d_c where $E < E_{pass}$ since IR > $\Delta\phi^*$. (b) anodic polarization curve of the sample in the crevice solution. (c) a cross section micrograph of the crevice wall below d_c where crevice corrosion occurred (courtesy of K. Cho).

counter electrode. The crevice corrosion process may be explained by the potential distribution along the crevice wall (Fig. 1). Due to the electric

shield effect, the electrode potential at some distance into a sufficiently deep crevice always remains at the mixed or equilibrium potential in the crevice electrolyte, referred to as the limiting potential (12,13), irrespective of the more oxidizing potential at the outer surface. The latter is established either by a potentiostat or by the reduction of dissolved oxygen in the bulk solution at the passivated outer surface. Thus, along the crevice wall, the local electrode potential decreases gradually from the value at the crevice opening (the more oxidizing potential) to a less oxidizing potential inside the crevice. At a certain distance, d_c, where the electrode potential equals the passivation potential of the anodic polarization curve of the crevice electrolyte, the crevice wall changes its state from passive to active. Thus, active dissolution occursbeyond d_c to the distance where the potential decreases to the limiting potential. The crevice wall dissolution current is highest at distances slightly greater than d_c, corresponding to the peak current in the anodic polarization curve. This can be seen in cross sections of the crevice wall as shown in Fig. 1c where the penetration of the crevice corrosion is deepest just to the right of E_{pass}. Since this potential distribution is controlled by the IR drop of the dissolution current flowing out of the crevice (i.e., the IR drop within the crevice must exceed the difference between the sample's outer surface potential and the passivation potential, E_{pass}, of the crevice electrolyte polarization curve, IR > sf (Fig. 1), in order that crevice corrosion occurs), this process is referred to as IR induced crevice corrosion. The IR drop mechanism suggests: (1) Crevice corrosion is due to the macro corrosion cell involving well separated anodic and cathodic reactions occurring at very different electrode potentials. This is consistent with the generally accepted current understanding of crevice corrosion. (2) The highest metal dissolution rate within a crevice corresponds to the peak current of the crevicing electrolyte polarization curve. That is, the crevice corrosion current is the anodic dissolution rate at high anodic overpotentials within the active region, which is hundreds or even a thousand times larger than the corrosion rate at the limiting potential due to local micro corrosion cells deeper in the crevice or at the corrosion potential (or applied potential) existing at the outer surface in the passive region. The IR mechanism overcomes the difficulty of the traditional hydrolysis mechanism which is solely based on the composition changes of the solution, not considering the distribution of anodic overpotential on the crevice wall.

The IR-drop mechanism can satisfactorily explain the accelerating effect on crevice corrosion of the pH decrease (due to hydrolysis) and of the chloride ion build up in the crevice. The pH decrease of the crevice electrolyte and the chloride ion build up may always result in a higher peak current and a more noble passivation potential in the anodic polarization curve, which in turn increases the maximum anodic dissolution rate on the crevice wall (IR increases) and decreases the Df value. Consequently, the total crevice corrosion current increases. The increase in IR and decrease in Df both lead to a decrease in the d_c value.

CRITICAL DISTANCE INTO THE CREVICE, d_c

The critical distance into the crevice, d_c, at which the crevice wall changes its state from passive into active, has a specific meaning for crevice corrosion. When the depth of a crevice is less than the maximum critical distance under the specified conditions, the crevice wall will be

fully passivated and no crevice corrosion occurs. On the other hand, when the depth is larger than the maximum critical distance, the crevice will be active at distances into the crevice greater than the d_c distance. It has been found, in both experiments and computations [15-19], that the critical distance into the crevice, d_c, is affected by several parameters as shown in Figs. 2 and 3. The crevice gap dimension has a remarkable influence on d_c. The larger the crevice gap, the larger the d_c (Fig. 2a). On the other hand, the crevice depth, d_o, has a weak influence and d_c, with d_c increasing slightly as d_o decreases to the d_c value, i.e., the maximum d_c occurs for d_c = d_o [14]. The magnitude of the passive current density affects d_c to a less extent than the gap dimension, with a larger passive current giving rise to a smaller d_c (Fig. 2b). A high solution conductivity decreases the resistance and so increases d_c (Fig. 2c). Also the higher (more oxidizing) the electrode potential (produced by an oxidant or power supply) at the sample's outer surface, the larger the d_c. An almost linear relationship exists between d_c and the outer surface electrode potential (Fig. 3). In addition the anodic behaviour of the metal, especially the peak current in the anodic polarization curve, has been found to significently influence d_c. To have the same critical distance for a larger crevice gap requires a higher peak current density for otherwise identical conditions [18]. All these relations are fully compatible with the IR drop mechanism.

The above factors affecting d_c are surprisingly consistent with those factors which are known, by experience and past research work, to influence the crevice corrosion resistance of materials. In the work by Fitzgerald and his predecessors [20-23], the crevice corrosion resistance has been found to increase with increasing crevice gap, passive potential range and solution conductivity but with decreasing peak current density of the anodic polarization curve and the active potential range. These are exactly the same factors affecting d_c described above. Therefore, it may be suggested to use the critical distance into the crevice, d_c, as the index of the crevice corrosion resistance of a material, i.e., the larger the d_c in a specified situation, the more resistant the material is to crevice corrosion.

The advantages of using d_c are apparent. First, it has a distinct and straightforward meaning. That is, d_c is the distance into a crevice beyond which crevice corrosion occurs. Secondly, d_c may be used in corrosion prevention design. As stated before, when the depth of an existing crevice d_o, is less than d_c for the specified conditions, the crevice will be in the passive state and so it can be tolerated. But when d_o is larger than d_c, the crevice wall beyond d_c will be in the active state and crevice corrosion will occur down to the of the limiting potential. A Nomograph or table of the relationship between d_c and the crevice geometry in a specified environment/metal combination may be prepared by computations (as explained later) and experiments. By referring to the graph or table, one may find out whether a crevice is safe (no crevice corrosion) or not. Thirdly, d_c is a single parameter to represent the crevice corrosion resistance. It combines the comprehensive effects of the several factors affecting the crevice corrosion resistance (the peak current density, the solution conductivity, the passive potential, etc.).

EXPERIMENT FOR MEASURING d_c

The experimental set up for measuring d_c is given in Fig. 4a. It consists of a three electrode corrosion cell, a potentiostat and a current recording device. The working electrode is made of the material to be tested. An artificial crevice is made on it. Two kinds of artificial crevice may be used: the straight crevice (Fig. 4b) and the cylindrical crevice
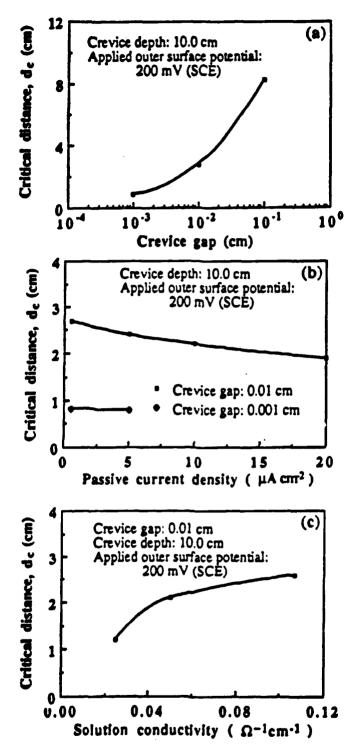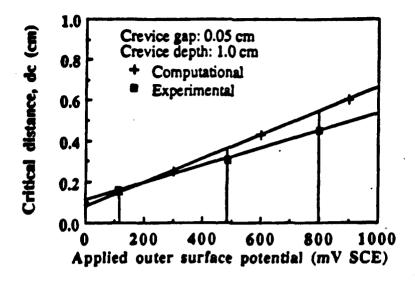
Fig. 2 The critical distance into the crevice, d_c, as a function of the (a) crevice gap dimension, (b) passive current density, and (c) solution conductivity.
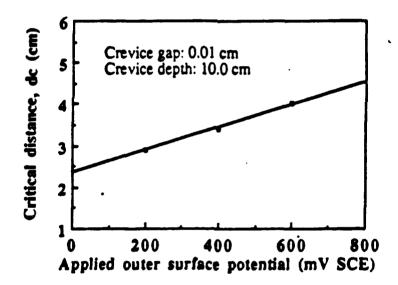
Fig. 3 Effect of the applied potential at the sample's outer surface on the
critical distance into the crevice, d_c. (a) High purity iron in a 0.5 M
acetic acid + 0.5 M sodium acetate solution. Computation results are in good
agreement with the experiments. (b) High purity iron in 1 M ammonia
hydroxide + 1 M ammonia nitrate.

(Fig. 4c). The former has been used for a long time in the Corrosion Laboratory of the Department of Materials Science and Engineering, The Pennsylvania State University. The straight crevice is made of a flat pyrex sheet on which a groove, 0.5 cm x 1.0 (or longer, say 2.0) cm x g, was cut, where g is the crevice gap dimension which can be made as small as 25 mm. The grooved face of the pyrex sheet is pressed against the flat surface of the sample. Thus, an artificial crevice of dimensions 0.5 cm x 1.0 cm (or longer) x g cm is formed. One advantage of using the straight crevice is that a camera may be installed in front of the pyrex sheet so that the crevice corrosion process may be observed and recorded in situ [17]. The cylindrical crevice is made of a hole drilled into a bulk component and a core component which is to be inserted into the hole. The core component may be positioned in the center of the hole by an orifice. The crevice is formed between the walls of the hole and the core. The bulk component is made of the testing metal or alloy and the core is made of an insulating high polymer, or the opposite. Alternatively, both the bulk and the core components may be made of the material to be tested. This device is similar to that used by France and Greene [23]. By adjusting the diameters of the hole and the core, the crevice gap may be adjusted.

The Luggin probe is placed close to the crevice opening to minimize the IR drop between the sample's outer surface and the opening of the capillary. This is particularly important when the solution conductivity is low. The area of the counter electrode should be large enough to make the potential distribution at the sample's outer surface more uniform so that the electrochemical test may best simulate the actual crevice corrosion situation in the natural environment. The test solution can be the one in which the metal is immersed during its service or a specially prepared corrosive solution for accelerating the test. The applied potential at the sample's outer surface must be within the passive region of the anodic polarization curve of the tested material. For comparison of different materials, the applied potential and the crevice gap dimension should be the same. The total current of the circuit is monitored from the beginning of the test. It takes a few hours for the current (which is mainly the current flowing out of the crevice) to reach a relatively stable value. After a period of time (one or two days if the peak current is large, or one or two weeks if the peak current is low), the experiment is terminated and the crevice wall or cross section is checked in an optical microscope to measure the critical distance. Sometimes the current declines to a very low value after an initial high reading, indicating that the crevice has become passivated. For some material/environment combinations, e.g., 304 stainless steel in sea water, the anodic polarization curve does not exhibit an active-passive transition and so the initial current reading is low. It takes longer time for the acidification and chloride on buildup to occur, and then the crevice corrosion current increases with time.

In the steady state, the potential distribution in the system observes the Laplace equation. For a straight crevice, in Cartesion coordinates, it is written as

$$\frac{\partial^2 \varphi}{\partial x^2} + \frac{\partial^2 \varphi}{\partial y^2} = 0$$
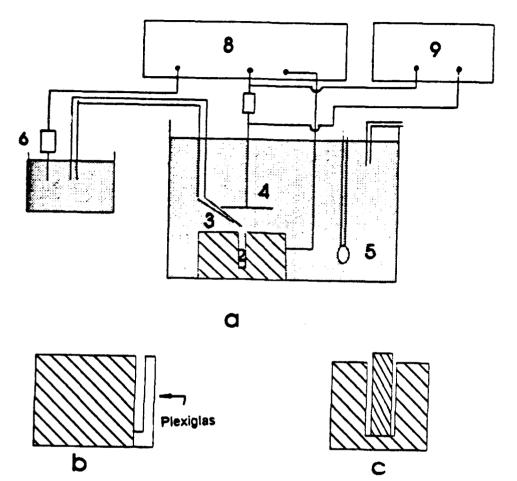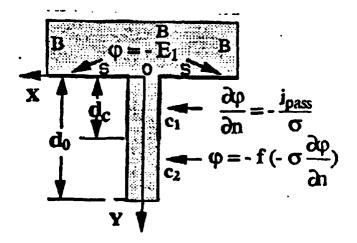
Fig. 4 (a) Experimental set up for measuring the critical distance into the crevice, d_c: 1.working electrode (the sample); 2. crevice; 3. Luggin capillary; 4. counter electrode; 5. gas purger; 6. reference electrode; 7. precision resistor for current measurement; 8. potentiostat; 9. pen recorder. (b) straight crevice with transparent (Plexiglas) wall. (c) cylindrical crevice.

For a cylindrical crevice, in cylindrical coordinates, the Laplace equation has the following form:

$$\frac{\partial^2 \varphi}{\partial 1^2} + \frac{1}{1}\frac{\partial \varphi}{\partial r} + \frac{\partial^2 \varphi}{\partial z^2} = 0$$

ESTIMATION OF d_c BY COMPUTATION

Another advantage of using d_c is that it can be estimated by computation. The coordinate system for the computation is shown in Fig.5.

Fig. 5. (a) Boundary conditions for the computation of d_c (Cartesian coordinates, straight crevice). (b) Boundary conditions for the computation of d_c (cylindrical coordinates, cylindrical crevice).

The boundary condition at the sample's outer surface (S in Fig. 5) is:

$$\varphi s = -E_1$$

where E_1 is the applied potential at the sample's outer surface. Along boundaries encircling the system (B in Fig. 5), the boundary condition is:

$$\left(\frac{\partial \varphi}{\partial n}\right)_{s} = 0$$

In the upper part of the crevice wall (passivated part, C_1 in Fig. 5), the boundary condition is:

$$\left(\frac{\partial \varphi}{\partial n}\right)_{c1} = -\frac{i_{pass}}{\sigma}$$

where i_{pass} is the passive current and σ is the solution conductivity. In the bottom part of the crevice (active dissolution part, C_2 in Fig. 5), the boundary condition becomes:

$$\varphi_{c2} = -E_{c2} = f(i_{c2}) = f\left(-\sigma\frac{\partial \varphi_{c2}}{\partial n}\right)$$

where $E_{c2} = f(i_{c2})$ is the active loop portion of the anodic polarization curve. This boundary condition is non linear with respect to the potential and its gradient.

The above Laplace equation contains a non linear boundary condition and so can not be solved by conventional numerical methods. A boundary variation and trial and error technique may be used to solve the problem. The full details of the computation method have been given elsewhere [14-16]. The solution of the Laplace equation is the potential distribution in the system, including on the crevice wall. Thus the critical distance into the crevice, d_c , where the potential is decreased to the passivation potential, E_{pass}, may be obtained. From the potential distribution and the polarization curve, the current distribution along the crevice may be determined. Then by integration, the total crevice corrosion current, I, may also be calculated. Preliminary computation has shown good agreement between the computed and the experimental values. Tables 1 and 2 and Fig. 2a are comparisons of the computation results with experiments for high purity iron in an acetic acid buffer solution [16].

TABLE 1. Comparison between the computational [15,16] and experimental data [16,18] of the critical crevice distance into the crevice, d_c, and the total crevicing current, I, for pure iron in 0.5 M acetic acid + 0.5 M sodium acetate solution. Crevice gap: g = 0.05 cm; applied potential at the sample's outer surface: E_1 = 115 mV (SCE); crevice length: 1 = 0.5 cm; crevice depth: d_0 = 1.0 cm.

Critical distance, d_c (cm)		Total crevicing current, I (mA)	
Computational	Experimental	Computational	Experimental
0.14	0.12-0.20	1.2	1.2-1.4

It is noted here that the above computation can only give an estimation of the d_c because of two reasons. (1) the polarization curve of the crevice electrolyte should be used in the computation. If the polarization data for the bulk solution is used, the obtained d_c is accurate only at the beginning of the crevice corrosion process when the composition of the crevice solution has not changed appreciably. With the progress of crevice corrosion, the composition and pH of the crevice electrolyte change with time and so does d_c. (2) The shape of the crevice changes with time due to corrosion so that the boundary condition on the crevice wall should also be changed with time. Thus, using the original boundary condition results in additional errors in d_c. Therefore, although the computation can sometimes give a good estimation of d_c, it can not replace the experiment.

TABLE 2. Comparison between the computational and experimental data of the critical distance into the crevice, d_c, for high purity iron on 0.5 M acetic acid + 0.5 M sodium acetate solution at different applied potentials, E_1, at the sample's outer surface. Crevice gap: $g=0.05$ cm; crevice depth: d_o - 1.0 cm.

Applied potential, E_1 (mV SCE)	Critical distance, d_c (cm)	
	Computational	Experimental
115	0.14	0.12-0.20
485	0.37	0.29-0.31
801	0.55	0.41-0.45

SUMMARY

A new index for the corrosion resistance of materials - the critical distance into the crevice, d_c - has been proposed. At d_c the local potential of the crevice wall is the passivation potential in the anodic polarization curve of the material in the crevice electrolyte. At greater distances, the crevice undergoes active anodic dissolution (crevice corrosion) down to the distance of the limiting potential. The larger the d_c, the better the crevice corrosion resistance of the material. Two artificial crevice designs have been introduced which can be used to measure the critical distance into the crevice. The d_c may also be estimated through computation. The advantages in using d_c as the index of crevice corrosion resistance have been discussed.

ACKNOWLEDGEMENT

REFERENCES

[1] "Standard Guide for Crevice Corrosion Testing of Iron-Base and Nickel-Base Stainless Alloys in Seawater and other Cloride-Containing Aqueous Environments", American Society for Testing and Materials, Annual Book of ASTM Standards, 03.02, G78

[2] A. H. Tuthill, "Resistance of Highly Alloyed Materials and Titanium to Localized Corrosion in Bleach Plant Environments", Mater. Perform., Vol. 24, October, 1985, pp. 43-49

[3] "Standard Test Methods for Pitting and Crevice Corrosion Resistance of Stainless Steels and Related Alloys by use of Ferric Chloride Solution", American Society for Testing and Materials, Annual Book of ASTM Standards, 03.02, G48

[4] R. S. Treseder and E. A. Kachik, Laboratory Corrosion Tests and Standards, STP 866, American Society for Testing and Materials, 1985, 373

[5] D. B. Anderson, "Statistical Aspects of Crevice Corrosion in Seawater", Galvanic and Pitting Corrosion - Field and Laboratory Studies, STP 576, American Society for Testing and Materials, Philadelphia, Pa., 1976, 231-242.

[6] "Standard Test Method for Conducting Cyclic Potentiodynamic Polarization", American Society for Testing and Materials, Annual Book of ASTM Standards, 03.02, G61

[7] "Standard Test Method for Pitting or Crevice Corrosion of Metallic Surgical Implant Materials", American Society for Testing and Materials, Annual Book of ASTM Standards, 03.02, F746

[8] S. Bernhardson, Paper 85, presented at Corrosion/80, Houston TX, NACE, 1980

[9] J. W. Oldfield and W. H. Sutton, "Crevice Corrosion of Stainless Steel", Br. Corros. J., Vol. 13, 1978, pp. 104-111.

[10] T. S. Lee, Electrochemical Corrosion Testing, STP 727, American Society for Testing and Materials, 1981, 43

[11] M. G. Fontana, Corrosion Engineering, 3rd Ed., McGraw-Hill, New York, 1986.

[12] H. W. Pickering, "Significance of the Local Electrode Potential Within Pits, Crevices and Cracks", Corrosion Sci. Vol. 29, 1989, pp. 325-341.

[13] H. W. Pickering, "On the Roles of Corrosion Products in Local Cell Processes", Corrosion, Vol. 42, March, 1986, pp. 125-140.

[14] Yuan Xu, Minghua Wang and H. W. Pickering, "A Mechanism of Pitting Corrosion", Oxide Films on Metals and Alloys, Electrochemical Soc., Pennington, NJ, in press.

[15] Yuan Xu and H. W. Pickering, "The Initial Potential and Current Distribution in the Crevice Corrosion Process", J. Electrochem. Soc., in press.

[16] Yuan Xu and H. W. Pickering, "A Model of the Potential and Current Distributions Within Crevices and Its Application to the Iron-Ammoniacal System", Critical Factors in Localized Corrosion, G. S. Frankel and R. C. Newman, eds., The Electrochem. Soc., Princeton, NJ, 1991, pp. 389-406; K. Cho and H. W. Pickering, ibid., pp. 407-419.

[17] K. Cho and H. W. Pickering, "The Role of Chloride Ions in the IR>IR* Criterion for Crevice Corrosion, J. Electrochem. Soc., Vol. 138, October, 1991, pp. L56-L58.

[18] K. Cho, MS Thesis, The Pennsylvania State University, 1991.

[19] K. Cho, PhD Thesis, The Pennsylvania State University, 1992.

[20] B. J. Fitzgarald, Thesis, University of Connecticut, 1976

[21] C. Edeleanu and J. G. Gibson, Chem. & Ind., 1961, pp. 301-.

[22] M. N. Folkin and V. A. Timonin, Dokl. Akad. Nauk. SSSR, Vol. 164, 1965, pp. 150-153.

[23] W. D. France and N. D. Greene, "Passivation of Crevices During Anodic Protection", Corrosion, Vol. 24, 1968, pp. 247-251.

Technical Reports and Publications   Feb 1990

Organization	Copies	Organization	Copies
Defense Documentation Center Cameron Station Alexandria, VA 22314	12	Naval Air Propulsion Center Trenton, NJ 08628 ATTN: Library	1
Office of Naval Research Dept. of the Navy 800 N. Quincy Street Arlington, VA 22217 ATTN: Code 1131	3	Naval Civil Engineering Laboratory Port Hueneme, CA 94043 ATTN: Materials Div.	1
Naval Research Laboratory Washington, DC 20375 ATTN: Codes 6000 6300 2627	1 1 1	Naval Electronics Laboratory San Diego, CA 92152 ATTN: Electronic Materials Sciences Division	1
Naval Air Development Center Code 606 Warminster, PA 18974 ATTN: Dr. J. DeLuccia	1	Commander David Taylor Research Center Bethesda, MD 20084	1
Commanding Officer Naval Surface Warfare Center Silver Spring, MD 20903-5000 ATTN: Library Code R33	1 1	Naval Underwater System Ctr. Newport, RI 02840 ATTN: Library	1
Naval Ocean Systems Center San Diego, CA 92152-5000 ATTN: Library	1	Naval Weapons Center China Lake, CA 93555 ATTN: Library	1
Naval Postgraduate School Monterey, CA 93940 ATTN: Mechanical Engineering Department	1	NASA Lewis Research Center 21000 Brookpark Road Cleveland, OH 44135 ATTN: Library	1
Naval Air Systems Command Washington, DC 20360 ATTN: Code 310A Code 5304B Code 931A	1 1 1	National Institute of Standards and Technology Gaithersburg, MD 20899 ATTN: Metallurgy Division Ceramics Division Fracture & Deformation Division	1 1 1

Office of Naval Research
Resident Representative
Ohio State University Research Center
1960 Kenny Rd
Columbus, OH 43210-1063

Naval Facilities Engineering
 Command
Alexandria, VA 22331
ATTN: Code 03   1

DOD Metals Information Analysis Center (MIAC)
CINDAS/Purdue University
2595 Yeager Road
West Lafayette, Indiana 47906-1398

Commancant of the Marine Corps   1
Scientific Advisor
Washington, DC 20380
ATTN: Code AX   1

Oak Ridge National Laboratory
Metals and Ceramics Div.
P.O. Box X
Oak Ridge, TN 37380   1

Army Research Office
P.O. Box 12211
Research Triangle Park, NC 27709
ATTN: Metallurgy & Ceramics
       Program   1

Los Alamos Scientific Lab.
P.O. Box 1663
Los Alamos, NM 87544
ATTN: Report Librarian   1

Army Materials Technology Laboratory
Watertown, MA 02172-0001
ATTN: Research Program Office   1

Argonne National Laboratory
Metallurgy Division
 P.O. Box 229
Lemont, IL 60439   1

Air Force Office of Scientific
 Research
Building 410
Bolling Air Force Base
Washington, DC 20332
ATTN: Electronics & Materials
       Science Directorate   1

Brookhaven National Laboratory
Technical Information Division
Upton, Long Island
New York 11973
ATTN: Research Library   1

NASA Headquarters
Washington, DC 20546
ATTN: Code RM   1

Lawrence Berkeley Lab.
1 Cyclotron Rd
Berkeley, CA 94720
ATTN: Library   1

David Taylor Research Ctr
Annapolis, MD 21402-5067
ATTN: Code 281   1
       Code 2813   1
       Code 0115   1

Supplemental Distribution List   Feb 1990

Profs. G.H. Meier and F.S.Pettit
Dept. of Metallurgical and
Materials Eng.
University of Pittsburgh
Pittsburgh, PA 15261

Prof. H.K. Birnbaum
Dept. of Metallurgy & Mining Eng.
University of Illinois
Urbana, Ill 61801

Prof. H.W. Pickering
Dept. of Materials Science and Eng.
The Pennsylvania State University
University Park, PA 16802

Prof. D.J. Duquette
Dept. of Metallurgical Eng.
Rensselaer Polytechnic Inst.
Troy, NY 12181

Prof. D. Tomanek
Michigan State University
Dept. of Physics and Astronomy
East Lansing, MI 48824-1116

Dr. M. W. Kendig
Rockwell International Science Center
1049 Camino Dos Rios
P.O. Box 1085
Thousand Oaks, CA 91360

Prof. R. A. Rapp
Dept. of Metallurgical Eng.
The Ohio State University
116 West 19th Avenue
Columbus, OH 43210-1179

Dr. R. W. Drisko
Code L-52
Naval Civil Engineering Laboratory
Port Hueneme, CA 93043-5003

Dr. R.D. Granata
Zettlemoyer Center for Surface Studies
Sinclair Laboratory, Bld. No. 7
Lehigh University
Bethlehem, PA 18015

Dr. G. D. Davis
Martin Marietta Laboratories
1450 South Rolling Rd.
Baltimore, MD 21227-3898

Prof. P.J. Moran
Dept. of Materials Science & Eng.
The Johns Hopkins University
Baltimore, MD 21218

Prof. J. Kruger
Dept. of Materials Science & Eng.
The Johns Hopkins University
Baltimore, MD 21218

Dr. B.G. Pound
SRI International
333 Ravenswood Ave.
Menlo Park, CA 94025

Prof. C.R. Clayton
Department of Materials Science
& Engineering
State University of New York
Stony Brook
Long Island, NY 11794

Dr. J. W. Oldfield
Cortest Laboratories Ltd
23 Shepherd Street
Sheffield, S3 7BA, England

Prof. Boris D. Cahan
Dept. of Chemistry
Case Western Reserve Univ.
Cleveland, Ohio 44106

Prof. G. Simkovich
Dept. of Materials Science & Eng.
The Pennsylvania State University
University Park, PA 16802

Prof. M.E. Orazem
Dept. of Chemical Engineering
University of Florida
Gainesville, FL 32611

Dr. P. S. Pao
Code 6303
Naval Research Laboratory
Washington, D.C. 20375

Dr. M. S. Bornstein
United Technologies Research Center
East Hartford, CT 06108

Prof. R. M. Latanision
Massachusetts Institute of Technology
Room 8-202
Cambridge, MA 02139

Dr. R. E. Ricker
National Institute of Standards and
 Technology
Metallurgy Division
Bldg. 223, Room B-266
Gaithersburg, MD 20899

Dr. F. B. Mansfeld
Dept. of Materials Science
University of Southern California
University Park
Los Angeles, CA 90089

Dr. W. R. Bitler
Dept. of Materials Sci. and Eng.
115 Steidle Building
The Pennsylvania State University
University Park, PA 16802

Dr. S. Smialowska
Dept. of Metallurgical Engineering
The Ohio State University
116 West 19th Avenue
Columbus, OH 43210-1179

Dr. R. V. Sara
Union Carbide Corporation
UCAR Carbon Company Inc.
Parma Technical Center
12900 Snow Road
Parma, Ohio 44130

Prof. G.R. St. Pierre
Dept. of Metallurgical Eng.
The Ohio State University
116 West 19th Avenue
Columbus, Oh 43210-1179

Dr. E. McCafferty
Code 6322
Naval Research Laboratory
Washington, D. C. 20375

Prof. J. O'M. Bockris
Dept. of Chemistry
Texas A & M University
College Station, TX 77843

Dr. V. S. Agarwala
Code 6062
Naval Air Development Center
Warminster, PA 18974-5000

Prof. Harovel G. Wheat
Dept. of Mechanical Engineering
The University of Texas
ETC 11 5.160
Austin, TX 78712-1063

Prof. S. C. Dexter
College of Marine Studies
University of Delaware
700 Pilottown Rd.
Lewes, DE 19958